Quaternary Research 77 (2012) 445–455

Contents lists available at SciVerse ScienceDirect

Quaternary Research

journal homepage: www.elsevier.com/locate/yqres

The OSL chronology of eolian sand deposition in a perched dune field along the northwestern shore of Lower Michigan

Bradley E. Blumer [a], Alan F. Arbogast [b,*], Steven L. Forman [c]

[a] Geographic Information System and Earth Science Specialist, City of Janesville, WI, 53548, USA
[b] Department of Geography, Michigan State University, East Lansing, MI, 48824, USA
[c] Department of Earth and Environmental Sciences, The University of Illinois at Chicago, Chicago, IL, 60607, USA

ARTICLE INFO

Article history:
Received 6 June 2010
Available online 6 March 2012

Keywords:
Lake Michigan
Sand dunes
OSL dating

ABSTRACT

Extensive coastal dunes occur in the Great Lakes region of North America, including northwestern Michigan where some are perched on high (~100 m) bluffs. This study focuses on such a system at Arcadia Dunes and is the first to systematically generate optical ages from stratigraphic sections containing buried soils. Dune growth began ca. 4.5 ka during the Nipissing high lake stand and continued episodically thereafter, with periods of increased sand supply at ca. 3.5 ka and ca. 1.7 ka. The most volumetrically dominant phase of dune growth began ca. 1.0 ka and continued intermittently for about 500 years. It may have begun due to the combined effects of a high lake phase, potential changes in lake hydrodynamics with final isostatic separation of Lake Superior from Lakes Michigan and Huron, and increased drought and hydrologic variability associated with the Medieval Warm Period. Thus, this latest eolian phase likely reflects multiple processes associated with Great Lakes water level and climate variability that may also explain older eolian depositional events. Comparison of Arcadia ages and calendar corrected ^{14}C ages from previous studies indicate broad chronological agreement between events at all sites, although it appears that dune growth began later at Arcadia.

Introduction

Previous research and geomorphic setting

Coastal dunes are common around the world (Carter et al., 1990) and form through complex interactions related to sand supply, prevailing winds, water level fluctuations, and climate change (Bauer and Sherman, 1999). Although such dunes are usually associated with marine environments (e.g., Gares and Nordstrom, 1995; Clemmensen et al., 2001; Hesp, 2001; Walker et al., 2006; Martinho et al., 2010; Short, 2010; Tamura et al., 2011), numerous coastal dunes occur in the Great Lakes region of North America. Dunes along the eastern shore of Lake Michigan (Fig. 1) contain the largest volume of sand due to prevailing westerly winds, long fetch, and abundant sand supply (Arbogast et al., 2009). South of Manistee, large (up to ~60-m-high) dunes line the coast for many kilometers in transgressive complexes that mantle pro-glacial lake plains lying a few meters above lake level (Arbogast et al., 2002a; Hansen et al., 2002; Arbogast, 2009). In contrast, dune fields in the northwestern part of Lower Michigan are usually more isolated and thus distinct physical entities. Although some dunes lie on surfaces that lie near lake level, the most spectacular dune fields mantle coastal bluffs up to ~100 m high (e.g., Snyder, 1985; Loope and Arbogast, 2000).

The first study of bluff-top dunes was conducted by Dow (1937) who assessed the formation of what he called *perched dunes* associated with the Manistee Moraine. He proposed four hypothetical sources of sand for these systems, including 1) eolian sand blown upslope from littoral sources; 2) beach sand driven upslope by waves as lake level rises toward the bluff base; 3) sand originating from glacial sediments in bluff exposures; and 4) a complex interaction of the three. Dow (1937) believed that sandy glacial sediment exposed in the bluff face is the dominant source of eolian sand, with increased supply during high lake levels when the coastline is unstable due to wave erosion. Sand supply subsequently diminishes when lake levels fall.

Following Dow's (1937) seminal study, perched dunes in Michigan were largely ignored for about 50 years, when renewed interest focused on systematic dating (^{14}C) and associated geomorphic reconstructions. The first such study was conducted by Snyder (1985) at Sleeping Bear Dunes National Lakeshore (Fig. 1). Subsequently, Loope and Arbogast (2000) assessed a series of dunes scattered along that part of the coast, including the vicinity of Empire Bluffs. Research in Upper Michigan has focused on bluff-top dunes along the southern shore of Lake Superior at the Grand Sable dune field (Anderton and Loope, 1995) and Nodaway Point (Arbogast, 2000). A critical discovery is that these landscapes often contain several buried soils, which are important chronostratigraphic markers because they represent intervals of limited sand supply and dune stability. At each site, dunes mantle

* Corresponding author: Fax: +1 517 432 1671.
E-mail address: dunes@msu.edu (A.F. Arbogast).

0033-5894/$ – see front matter © 2012 University of Washington. Published by Elsevier Inc. All rights reserved.
doi:10.1016/j.yqres.2012.01.006

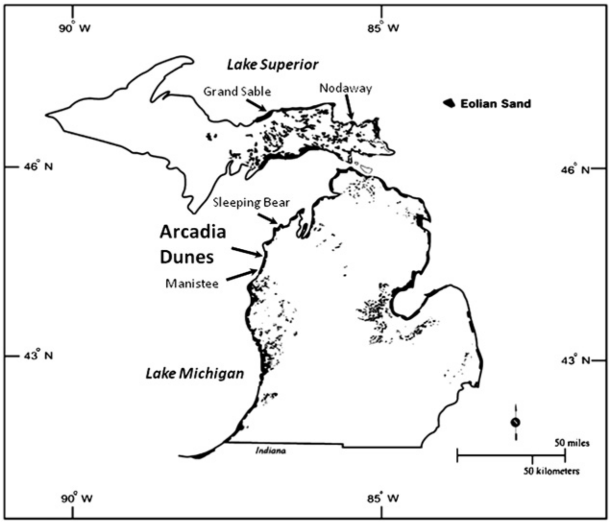

Figure 1. Distribution of eolian sand in Michigan. Extensive areas of dunes line the coasts of Lake Michigan, Lake Superior and Lake Huron. The highest concentration of dunes occurs along Lake Michigan. Dune fields mentioned in this report are identified (modified from Lepczyk and Arbogast, 2005).

a well-developed paleosol formed in the top of the underlying glacial sediments (Snyder, 1985; Anderton and Loope, 1995; Arbogast, 2000; Loope and Arbogast, 2000).

This basal paleosol apparently evolved during the early Holocene when lake levels were significantly lower because the eastern outlets were topographically low due to sill downcutting (Superior basin) and deglaciation of the isostatically depressed North Bay outlet (Michigan/Huron basin). This period of low lake level is called the Houghton stage and Chippewa stage in the Lake Superior and Lake Michigan basins, respectively (Larson and Schaetzl, 2001). Lake level remained low until the early part of the Nipissing transgression, which began about 9 ka in the Lake Michigan basin due to outlet rebound. Lake level peaked (~183 masl) during the Nipissing high stand at ca. 5 ka. Radiocarbon ages from the basal soils suggest that they were buried by eolian sand about this time (Snyder, 1985; Anderton and Loope, 1995; Loope and Arbogast, 2000). This age association may reflect coastal instability during the latter part of the Nipissing transgression, consistent with Dow's (1937) dominant mode of perched-dune growth.

Several buried soils have been recognized within the dunes that indicate variable sand supply in the late Holocene. At Sleeping Bear a pair of buried A horizons yielded uncalibrated ^{14}C ages of ca. 2800 and 700 ^{14}C yr BP (Snyder, 1985). At Grand Sable, a series of uncalibrated ^{14}C ages were obtained from buried soils that ranged from ca. 4000 to 500 ^{14}C yr BP (Anderton and Loope, 1995). In the vicinity of Empire Bluffs along Lake Michigan, four weakly developed buried soils provided ages ranging from ca. 3100 to 60 ^{14}C yr BP (Loope and Arbogast, 2000). Surprisingly, the bulk of eolian sand along the coast of northwest Lower Michigan, approximately 75% by volume, is <1500 years old (Loope and Arbogast, 2000).

Purpose of this study

Chronological constraint for eolian stratigraphic records of perched dune fields in Michigan is currently provided exclusively by uncalibrated ^{14}C ages derived from charcoal and wood in buried soils (Snyder, 1985; Anderton and Loope, 1995; Loope and Arbogast, 2000). It is assumed that these ages estimate the timing of soil burial, which may be erroneous given uncertainties associated with the residence time of organic residue (e.g., Bailey et al., 2001; Roberts and Plater, 2007) and dating uncertainties. Fortunately, a viable geochronologic alternative is optical stimulated luminescence (OSL) dating which has been used extensively in the past decade to reconstruct dune chronologies (e.g., Forman et al., 2001; Arbogast et al., 2002a, 2002b; Holmes et al., 2008; Forman et al., 2009).

In this study we systematically generate OSL ages for stratigraphic sections of eolian sand intercalated with buried soils to better assess linkages to lake level variability (e.g., Baedke and Thompson, 2000), regional drought (Booth et al., 2006a) and lake hydrographic changes (Johnston, et al., 2007). This history is compared with the previously uncalibrated chronology of perched dunes in the region (Snyder, 1985; Anderton and Loope, 1995; Loope and Arbogast, 2000) through systematic calendar correction of the original age data. As a result, this study sheds light on regional environmental variables responsible for perched dune growth in the Great Lakes region and provides a model for comparisons between OSL and uncalibrated radiocarbon chronologies in dune systems around the world.

Study area

This study focuses on the Arcadia dune field, which is a perched complex in northwest Lower Michigan (Fig. 1). The property is located just north of the Manistee-Benzie County border and is part of the *Arcadia Dunes Conservation Area*. Within this area, the dunes occur within an approximately 300-ha area between highway M-22 and the lakeshore (Fig. 2).

Most of the landforms surrounding the Arcadia Dunes were constructed during the late Wisconsin glaciation of Lower Michigan. The dunes are perched about 90 m above Lake Michigan on the Manistee Moraine (Dow, 1937), which is generally associated with the Greatlakean readvance of the Lake Michigan lobe about 14,000 years ago (Evenson et al., 1976; Larson and Schaetzl, 2001). The moraine is composed of sandy till and outwash contained within irregular ridges perpendicular to the shoreline (Leverett and Taylor, 1915; Farrand and Bell, 1982; Farrand, 1988; Blewett, 1990).

The Arcadia Dunes consist mostly of long ridges that run parallel to the shoreline (Fig. 2). Dow (1937: p. 430) named the major lakeward ridge *razorback*, which in turn contains a large blowout (that Dow called a *windrift*) extending inland about 400 m. The limbs of this blowout are locally called *Old Baldy*. Several stable, densely vegetated dune ridges occur northwest of Old Baldy and extend north to Herring Lake. Erosion of the dune ridges along the bluff has revealed a sequence of pedostratigraphic units in eolian sand that were the focus of this study.

The climate of the Mansitee-Benzie county area is classified as humid continental, with warm summers and cold winters. Monthly high temperatures at Manistee, (33 km south-southwest of the study area) range between −5.2°C in January to 20.7°C in July, with a mean of 8.1°C annually. Average annual precipitation is 78.5 cm and generally distributed uniformly throughout the year. Much of this precipitation is snowfall, which averages 234.2 cm/yr. Vegetation in the dune field ranges from marram grass (*Ammophila breviligulata*) on partially stabilized dunes to stands of American beech (*Fagus grandifolia*), sugar maple (*Acer saccharum*) and northern red oak (*Quercus rubra*) on fully stabilized dunes (Kroell, 2008).

Methods

Field methods

The stratigraphic and chronological relationships at Arcadia Dunes were assessed with a variety of techniques. Three exposures (Fig. 3) were identified for detailed analyses during field reconnaissance. Two of these exposures are located directly above the bluff face and are labeled Exposure 1 (southerly) and Exposure 2 (northerly). Exposure 3 is located in the southeastern edge of the large blowout in the dune field. Exposures 1 and 2 were subsequently described and measured with the aid of a homemade device designed for steep slopes.

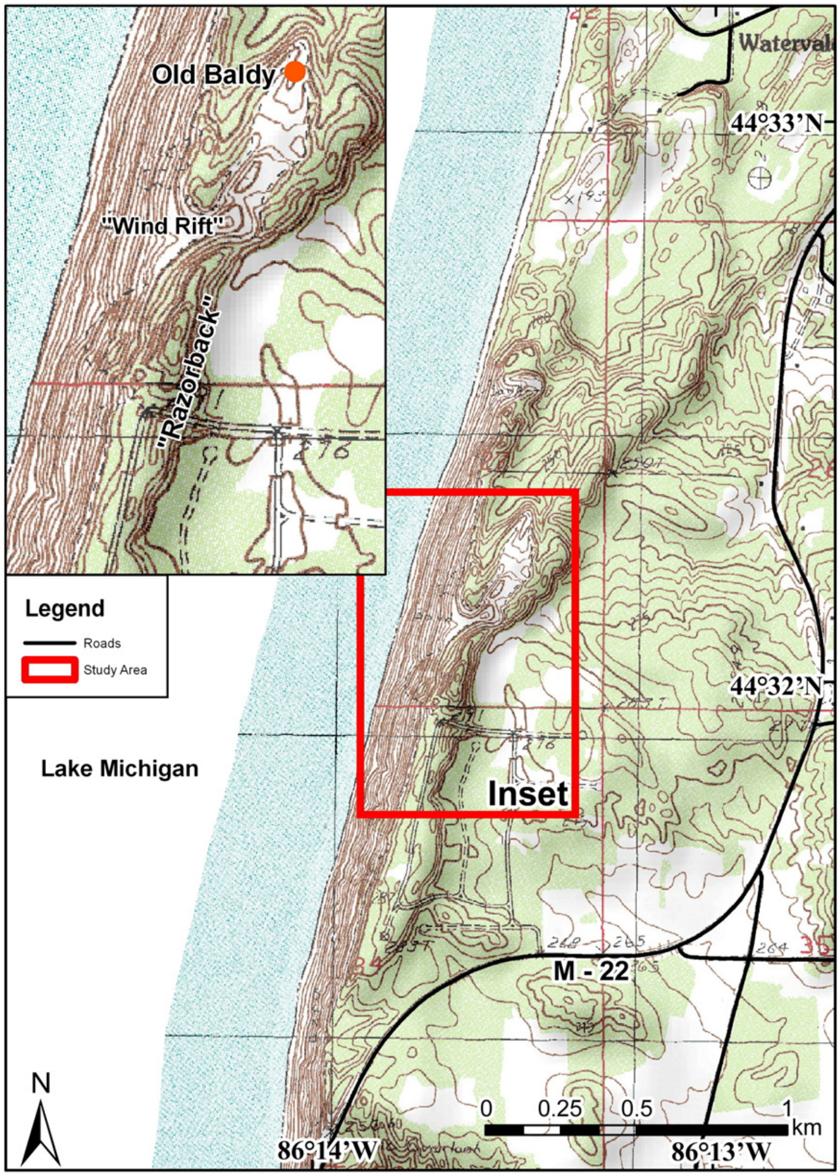

Figure 2. Topographic map of the study area (red). Focus box is on the landform feature names given by Dow (1937). Contour interval: 5 m.

This apparatus required three people and consisted of a 3-m pole used to form a right angle to a piece of measured string extended up the slope. One person held the pole plumb (with the use of a level) while another climbed upslope to measure the horizontal distance. The third person insured that the string formed a right angle by visually checking the string with a T-square affixed to the top of the pole. This technique was used to establish stratigraphic boundaries and to calculate their elevations above Lake Michigan. A USGS topographic map was used to estimate the elevation of the third exposure.

In the process of surveying site stratigraphy, special care was taken to identify and measure the elevation of outcropping buried soils. Such paleosols were cleaned and described for horizonation, thickness, and depth from the surface. A variety of samples were extracted for OSL dating from unaltered sands in distinct pedostratigraphic units using PVC pipe (72 cm long) to prevent light exposure. Each pipe was wrapped in electrical tape, driven into the cleaned face, and then sealed with duct tape upon extraction. A large amount of the surrounding sand was also collected to calculate the dose rate and moisture content of the host deposits. In the case of very thick eolian units, samples were collected from the upper and lower portions of the deposit to provide bracketing ages.

Optical dating

In this study only medium-to-fine eolian sand associated with primary dune bedforms was sampled for optical dating. Single Aliquot Regeneration (SAR) protocols (Murray and Wintle, 2003) were used to estimate the equivalent dose of the 100–150 μm quartz fraction for up to 41 separate aliquots (Table 1). Each aliquot contains ~2000 to 5000 quartz grains and was adhered to approximately 1-cm-diameter aluminum disc. This aliquot size was chosen to maximize light output for the natural with excitation; smaller aliquots (e.g., 0.5 cm) often yielded insufficient emissions. Eolian sands from coastal Michigan are mineralogically mature with SiO_2 content of >84%, and are predominantly (>80%) well-sorted quartz grains. The quartz fraction was isolated by density separations using the heavy liquid Na–polytungstate, and a 40-minute immersion in HF was applied to etch the outer ~10 μm of grains, which are affected by alpha radiation (Mejdahl and Christiansen, 1994). Quartz grains were rinsed finally in HCl to remove any insoluable fluorides. The purity of quartz separate was evaluated by petrographic inspection and point counting of a representative aliquot. Samples that showed >1% of non-quartz minerals were retreated with HF and rechecked petrographically. The

https://doi.org/10.1016/j.yqres.2012.01.006 Published online by Cambridge University Press

Figure 3. Aerial photograph of the study area showing the location of exposures where detailed descriptions and dating was conducted. "Old Baldy" is identified for reference.

purity of quartz separates was tested by exposing aliquots to infrared excitation which preferentially excites feldspar minerals. Samples measured showed weak emissions (<200 counts/second), at or close to background counts with infrared excitation, and ratio of emissions from blue to infrared excitation of >20, indicating a spectrally pure quartz extract (cf. Duller et al., 2003).

Blue light excitation (90% power at 470 ± 20 nm) from an Automated Risø TL/OSL–DA–15 system (Bøtter-Jensen et al., 2000) was used for SAR analyses. A Thorn EMI 9235 QA photomultiplier tube coupled with three 3-mm-thick Hoya U-340 detection filters, transmitting between 290 and 370 nm, measured photon emissions. Laboratory irradiations used a calibrated $^{90}Sr/^{90}Y$ beta source coupled with the Risø reader. All SAR emissions were integrated over the first 0.8 s of stimulation out of 50 s of measurement, with background based on emissions for the last 40- to 50-second interval (Fig. 4a). The luminescence emission for quartz sands showed a dominance of a fast component (cf. Murray and Wintle, 2003) with >90% diminution of luminescence after 4 seconds of excitation with blue light (Fig. Fig. 4a).

A series of experiments was performed to evaluate the effect of preheating at 180°, 200°, 220°, and 240°C on thermal transfer of the regenerative signal prior to the application of SAR dating protocols (c.f. Murray and Wintle, 2003). These experiments showed no preheat-based sensitivity changes and a preheat temperature of 220°C was used in SAR analyses. A test for dose reproducibility was also performed following procedures of Murray and Wintle (2003) with the initial and final regenerative dose of 2.23 Gy yielding concordant luminescence response (at 1-sigma error) (Fig. 4a). Dose recovery tests were performed on one represented sample (UIC2120) and the ratio of the applied and recovered dose is 0.97 ± 0.04 indicating that the SAR protocols accurately recover an applied dose (Fig. 5).

At least 41 aliquots were measured for each equivalent dose determination (Table 1). Equivalent dose distributions were log normal and unimodal (Fig. Fig. 4b) and thus, the central age model of Galbraith et al. (1999) was utilized for final equivalent dose calculation. Overdispersion values are between 15 and 30% for equivalent dose determinations, reflecting precision beyond instrumental errors. For each sample individual aliquots were eliminated from the final distribution and age determination if the recycling ratio was not between 0.90 and 1.10.

A determination of the environmental dose rate is a needed to render an optical age. This dose rate is an estimate of sediment exposure

Table 1
Single aliquot regeneration ages for the three exposures at the high-perched dunes at Arcadia Dunes in northwest Lower Michigan.

Laboratory #	Aliquots	Equivalent Dose (Gy)[a]	U (ppm)[b]	Th (ppm)[b]	K (%)[b]	Cosmic dose (Gy/ka)[c]	Dose rate (Gy/ka)[d]	SAR age (ka)[e]
Exposure 1								
UIC2128	32/40	0.96 ± 0.10	0.9 ± 0.1	3.1 ± 0.1	1.99 ± 0.02	0.18 ± 0.02	2.36 ± 0.11	0.410 ± 0.040
UIC2124	32/40	1.87 ± 0.19	0.8 ± 0.1	2.0 ± 0.1	1.97 ± 0.02	0.06 ± 0.01	1.91 ± 0.10	0.970 ± 0.010
UIC2121	39/40	3.34 ± 0.40	0.5 ± 0.1	1.7 ± 0.1	1.82 ± 0.02	0.04 ± 0.01	1.89 ± 0.10	1.765 ± 0.190
UIC2119	40/40	6.56 ± 0.66	0.7 ± 0.1	2.1 ± 0.1	1.72 ± 0.02	0.04 ± 0.01	1.88 ± 0.10	3.495 ± 0.335
UIC2118	40/40	10.15 ± 0.70	0.9 ± 0.1	2.9 ± 0.1	2.75 ± 0.02	0.02 ± 0.01	2.88 ± 0.14	3.530 ± 0.300
Exposure 2								
UIC2122	41/50	0.79 ± 0.18	0.6 ± 0.1	2.0 ± 0.1	2.30 ± 0.02	0.18 ± 0.02	2.49 ± 0.12	0.320 ± 0.050
UIC2123	29/40	1.30 ± 0.24	0.6 ± 0.1	2.0 ± 0.1	1.84 ± 0.02	0.15 ± 0.02	2.05 ± 0.10	0.630 ± 0.085
UIC2129	38/40	1.70 ± 0.24	0.7 ± 0.1	2.2 ± 0.1	2.28 ± 0.02	0.03 ± 0.01	2.38 ± 0.11	0.710 ± 0.080
UIC2125	39/40	2.39 ± 0.27	0.7 ± 0.1	2.6 ± 0.1	2.53 ± 0.03	0.03 ± 0.01	2.62 ± 0.13	0.910 ± 0.095
UIC2127	37/40	7.04 ± 0.51	0.5 ± 0.1	1.7 ± 0.1	1.54 ± 0.02	0.02 ± 0.01	1.62 ± 0.08	4.340 ± 0.380
UIC2120	40/40	12.64 ± 1.21	0.8 ± 0.1	2.9 ± 0.1	2.70 ± 0.02	0.02 ± 0.01	2.80 ± 0.14	4.500 ± 0.445
Exposure 3								
UIC2126	37/40	9.94 ± 0.94	0.6 ± 0.1	1.9 ± 0.1	2.26 ± 0.02	0.17 ± 0.02	2.44 ± 0.12	4.070 ± 0.380

[a]Equivalent dose determined by the single aliquot regenerative dose method under blue light excitation (470 nm) (Murray and Wintle, 2003) on the 150–250 μm quartz fraction. Central age model of Galbraith et al. (1999) was used.
[b]U, Th and K values determined by ICP-MS, Activation Laboratory Ltd., Ontario.
[c]Contains a cosmic rate dose rate component from Prescott and Hutton (1994).
[d]A long-term moisture content of 5 ± 2% was assumed.
[e]All errors are at one sigma include systematic and random components and ages are from reference year AD 2000. Analyses preformed by Luminescence Dating Research laboratory, Dept. of Earth & Environmental Sciences, Univ. of Illinois-Chicago.

to ionizing radiation from U and Th decay series, ^{40}K, and cosmic sources during the burial period (Table 1). The U and Th content of the dose rate samples, assuming secular equilibrium in the decay series and ^{40}K, were determined by inductively coupled plasma-mass spectrometry analysed by Activation Laboratory LTD, Ontario, Canada. The beta and gamma doses were adjusted according to grain diameter to compensate for mass attenuation (Fain et al., 1999). A small cosmic ray component between 0.18 and 0.02 mGy/yr, depending on depth of sediment, was included in the estimated dose rate (Prescott and Hutton, 1994). A moisture content (by weight) of 5 ± 2% was assumed.

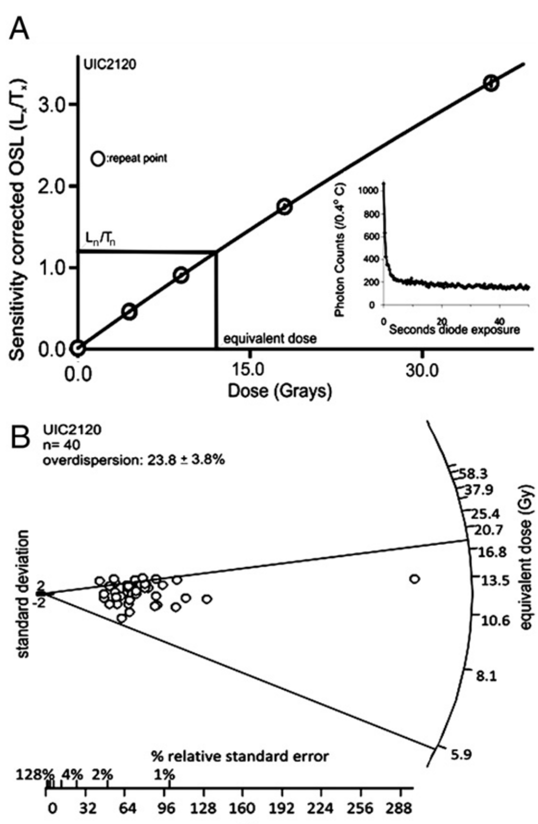

Figure 4. Luminescence data for the 100–150 micron quartz aliquots for sample UIC2120 (A).Dose response curve showing L_n/T_n ratio and associated equivalent dose. Inset figure shows typical natural luminescence shine down curve with exposure to light from blue emitting diodes (470 +/− 20 nm). (B) Radial plot of equivalent dose data for UIC2120; lines forming the wedge indicates two sigma limit.

Results and discussion

Site stratigraphy and OSL Ages

This section discusses the chronostratigraphy at each of the study exposures at Arcadia Dunes. These results are placed subsequently within the context of paleoenvironmental records (e.g., Booth et al., 2006a), the perched-dune model (Dow, 1937), reconstructed lake-level fluctuations (e.g., Thompson and Baedke, 1999; Baedke and Thompson, 2000), lake hydrodynamic changes (Johnston et al., 2007), and other perched dune fields in Michigan (e.g., Snyder, 1985; Loope and Arbogast, 2000).

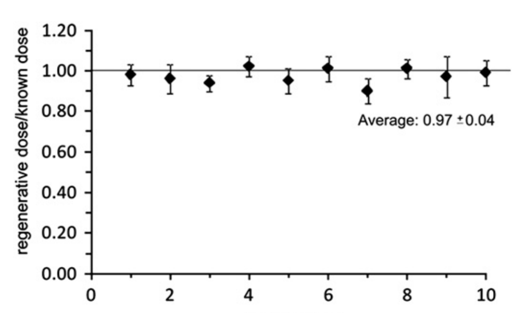

Figure 5. Dose recovery test for UIC2120 with a ratio of 1.00 indicating 100% recovery of dose. The average dose recovery for ten discs is 0.97 ± 0.04, indicating that SAR protocols can accurately recover an applied dose.

https://doi.org/10.1016/j.yqres.2012.01.006 Published online by Cambridge University Press

Exposure 1

Exposure 1 is located in the southern part of the study area (Fig. 3). This exposure is about 130 m tall, extending from the beach to the dune top where it reaches an elevation of 310 masl. The exposure slope is approximately 61% (Fig. 6). The basal unit (Unit I) consists of undifferentiated glacial sediment, consisting of mixed sand and gravel, that extends from the beach to about 100 m above lake level (Fig. 7). An Entisol is formed at the top of the glacial sediments. This soil is trending towards a Spodosol and is covered by about 28 m of eolian sand. An abrupt shift from coarse glacial sand and gravel to fine, well-sorted eolian medium sand marks this contact. Contained within the eolian sands are six pedostratigraphic units bounded by paleosols. Formed in the lowermost 33 cm of the eolian sand are two Entisols formed in Units II and III, respectively (Fig. 7). These Entisols are buried by Unit IV, a relatively thick (11.8 m) deposit of fine sand. Quartz grains from near the base (27.95 m) and top (16.31 m) of this deposit yielded OSL ages of 3.495 ± 0.335 ka (UIC 2119) and of 3.53 ± 0.3 ka (UIC 2118), respectively. An Entisol with spodic characteristics is formed in the uppermost part of Unit IV.

Unit V overlies Unit IV and consists of a thin (~1 m) unit of well-sorted fine sand that returned an OSL age of 1.765 ± 0.19 ka (UIC 2121) from quartz grains (14.86 m). A well-developed Entisol is formed at the top of unit V. This soil is buried by 14 m of very well-sorted fine sand (Unit VI) from which quartz grains near the base (14.23 m) and top of unit (1.32 m) gave OSL ages of 0.970 ± 0.1 ka (UIC 2124) of 0.4 ± 0.04 ka (UIC 2128), respectively. An Entisol with spodic characteristics occurs at the uppermost part of Unit VI, which is buried by 22 cm of fine sand that extends to the surface.

Exposure 2

Exposure 2 is located in the central part of the study area (Fig. 3) approximately 600 m north-northeast of Exposure 1. This exposure is about 115 m high, extending from the beach to the top of the dune where it reaches an elevation of 295 masl. The slope of Exposure 2 is approximately 56% (Fig. 6).

Exposure 2 contains eleven pedostratigraphic units (Fig. 8). The basal unit (Unit I) consists of undifferentiated glacial sand and gravel extending from the beach to a height of about 85 m above the lake. An Entisol with spodic characteristics is formed at the top of the glacial sediments. Overlying these sediments is about 26 m of eolian sand. As at Exposure 1, the contact between the glacial and eolian deposits is marked by an abrupt textural change.

Contained within the eolian sands are ten stratigraphic units that are bounded by paleosols. The basal eolian unit (Unit II) consists of about 7 cm of fine sand in which an Entisol has formed. This soil is buried by Unit III, a 4.5 m thick deposit of fine sand. Quartz grains from near the base (25.58 m) and top (21.67 m) of the deposit yielded OSL ages of 4.5 ± 0.445 ka (UIC 2120) and of 4.34 ± 0.380 ka (UIC 2127), respectively. A well-developed Entisol, one trending toward a Spodosol, is formed at the top the eolian unit.

A thin (~1 m) unit of fine sand (Unit IV) lies above the Entisol. Quartz grains at a depth of 20.55 m gave an OSL age of 0.91 ± 0.095 ka (UIC 2125). Formed at the top of this unit is an Entisol that is, in turn, buried by an 18-m-thick unit of fine sand (Unit V). Quartz grains near the base (19.92 m) and top (2.6 m) of Unit V returned OSL ages of 0.71 ± 0.08 ka (UIC 2129) and of 0.63 ± 0.085 ka (UIC 2123), respectively. An Entisol is formed in the top of this unit.

Overlying Unit V is a sequence of seven closely spaced deposits of eolian sand that are separated by very weakly developed soils (Fig. 8). The series begins with three Entisols separated by thin units of eolian sand, ranging from 9 to 30 cm thick. A 36-cm-thick

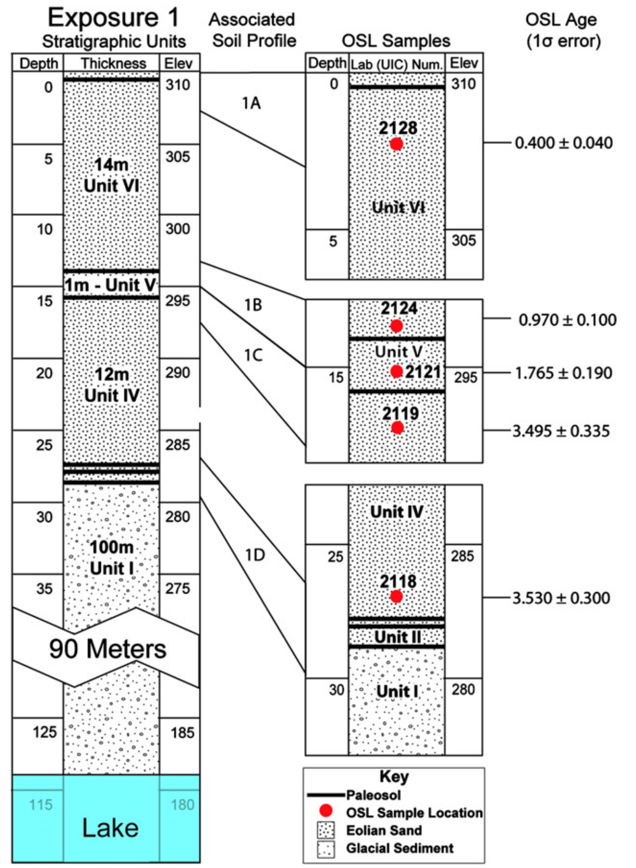

Figure 7. Generalized stratigraphy of Exposure 1. Major eolian units and paleosols are shown in relation to their associated soil profile. Generalized OSL sample locations are labeled with UIC sample number and associated age (in ka). Depth and elevation in meters.

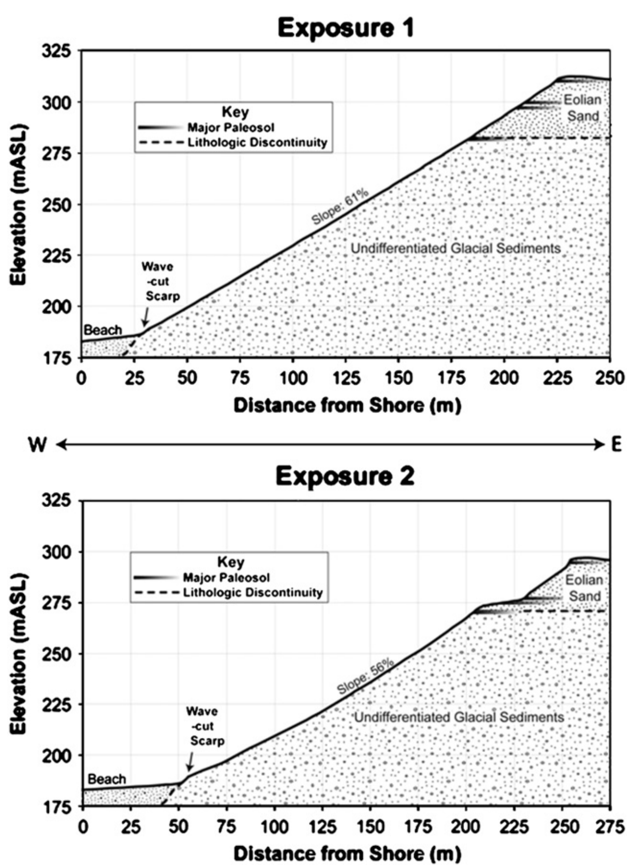

Figure 6. Profile view and general stratigraphy of the two lake-facing bluff exposures.

https://doi.org/10.1016/j.yqres.2012.01.006 Published online by Cambridge University Press

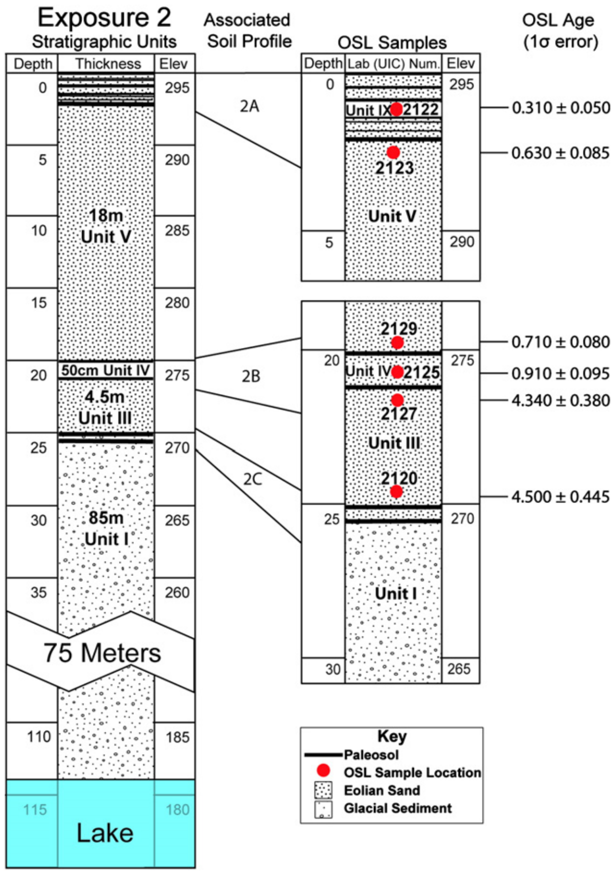

Figure 8. Generalized stratigraphy of Exposure 2. Major eolian units and paleosols are shown in relation to their associated soil profile. Generalized OSL sample locations are labeled with UIC sample number and associated age (in ka). Depth and elevation in meters.

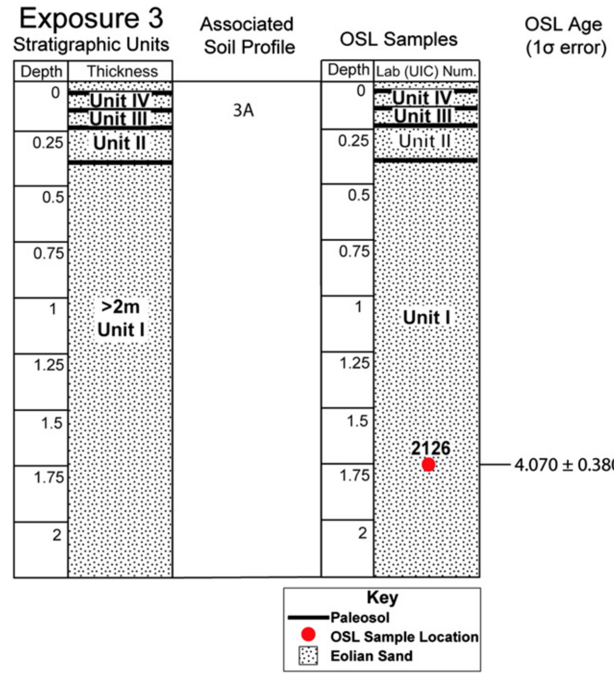

Figure 9. Generalized stratigraphy of Exposure 3. Major eolian units and paleosols are shown in relation to their associated soil profile. The OSL sample location is labeled with UIC sample number and associated age (in ka). Depth and elevation in meters.

deposit of fine sand overlies these soils, which yielded the OSL age of 0.31 ± 0.05 ka (UIC 2122) from quartz grains. Formed in this unit of fine sand is an Entisol, which in turn is buried by two other thin units of fine sand in which Entisols formed, including one at the modern surface.

Exposure 3

Exposure 3 is located in the central part of the study area, approximately 150 m inland of the bluff exposures (Fig. 3). This site is southeast of the high ridge that contains Exposure 2 and is located within the edge of the prominent blowout. The elevation at the top of Exposure 3 is approximately 295 masl, which is similar as Exposure 2.

Exposure 3 contains five pedostratigraphic units formed in eolian sand (Fig. 9). The basal unit is about 1.4 m thick and consists of fine sand that gave an OSL age of 4.07 ± 0.38 ka (UIC 2126) from quartz grains at a depth of 1.75 m. Formed in the uppermost part of the unit is an Entisol with spodic characteristics. Above this basal unit is a series of thin eolian units ranging from 14 to 19 cm thick, in which Entisols have formed, including the modern surface soil.

Geomorphic history of Arcadia dunes and regional comparisons

Stratigraphic analyses and associated OSL dating of pedostratigraphic units at Arcadia Dunes is the basis for inferring periods of eolian activity in the late Holocene. These results indicate that the lower ~75% of the bluff exposures are undifferentiated glacial sediments that were likely deposited during the Greatlakean readvance ca. 14,000 ka (Larson and Schaetzl, 2001). This stratigraphic setting was first noted by Dow (1937) and is consistent with relationships at other perched dune systems in the region (Snyder, 1985; Anderton and Loope, 1995; Loope and Arbogast, 2000).

Evidence indicates that the Arcadia landscape was stable for a prolonged period following glacial deposition, resulting in the development of a soil with spodic characteristics. This period of stability has also been recognized at other perched systems (Snyder, 1985; Anderton and Loope, 1995; Loope and Arbogast, 2000). According to Snyder (1985), this period of stability occurred during the Chippewa low stage during the early Holocene when the active shorezone was far away. Similar associations occur at Grand Sable (Anderton and Loope, 1995) and Nodaway (Arbogast, 2000) dune fields along the southern shore of Lake Superior (Fig. 1).

Evidence indicates that mobilization of eolian sand began at Arcadia Dunes ca. 4.5 ka during the Nipissing high stand (Fig. 10) and buried the glacial sediments. The onset of this depositional interval is marked by a thin (~7-cm-thick) deposit of eolian sand at Exposure 2 that contains a weakly developed Entisol. This soil was subsequently buried by a 4.5-m-thick deposit (Unit III) of eolian sand with bracketing OSL ages of ca. 4.5 and 4.3 ka from the lower and upper parts of the unit, respectively. These ages suggest a single depositional interval. An age of ca. 4.07 ka, which overlaps within one sigma with the basal ages at Exposure 2, was obtained from the blowout wall in Exposure 3. Eolian sand probably began to accumulate at Exposure 1 at this time as well, which is suggested by the thin units of basal eolian sand at this site. Initial growth of sand dunes during this time has also been reported along much of Lake Michigan's southeastern shoreline where numerous OSL and calibrated ^{14}C ages have been obtained (e.g., Arbogast and Loope, 1999; Arbogast et al., 2002a; Hansen et al., 2010).

Following the onset of dune growth at Arcadia, the next documented period of eolian activity was recognized at Exposure 1 in Unit IV at ca. 3.5 ka. Dune construction at this time has also been observed along the southeastern shore of Lake Michigan (e.g., Arbogast et al., 2002a; Hansen et al., 2010). This timing appears to correlate with a distinct regression in Lake Michigan (Fig. 10) that followed the Nipissing high stand (Baedke and Thompson, 2000). On the other hand, paleoecologic records from adjacent peatlands indicate

https://doi.org/10.1016/j.yqres.2012.01.006 Published online by Cambridge University Press

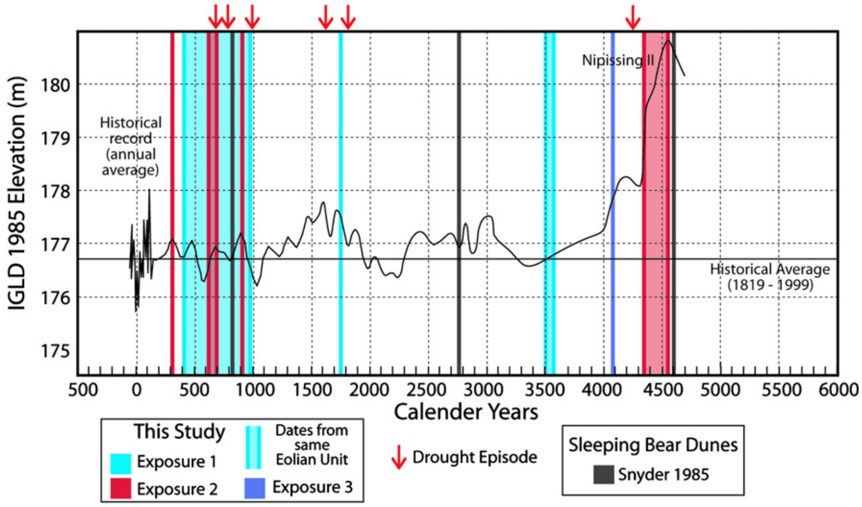

Figure 10. Dates of eolian activity correlated to a Holocene lake-level curve for Lake Michigan (Modified from Baedke and Thompson, 2000) and periods of drought reconstructed by Booth et al. (2006a). Age data from Sleeping Bear dunes (Snyder, 1985) are actually not calendar corrected, but are presented here to visualize the temporal correlation if OSL ages and uncalibrated ^{14}C ages are chronologically compared.

variable, but mostly wet hydrologic conditions on decadal to century timescales between ca. 3.9 and 3.0 ka (Booth et al., 2006a). This hydrologic variability may translate to decadal to century lake level variations, which may remain undetectable in the strandplain record of past lake level because of the century to millennial temporal resolution and restricted sub-meter elevational sensitivity (cf. Baedke and Thompson, 2000; Argyilan et al., 2005).

Following the period of dune growth at ca. 3.5 ka at Exposure 1, the landscape at Arcadia stabilized sufficiently for a well-developed Entisol with spodic characteristics to form. This soil apparently developed over a period of ca. 1700 years, as it was buried at ca. 1.76 ka by Unit V during a period of rising lake level (Fig. 10). The overall lack of dune growth at Arcadia during this time correlates reasonably well with a distinct period of stability between about 2.5 and 1 ka in dunes along the southeastern Lake Michigan shore, which resulted in formation of the prominent (A/E/Bs/C horizonation) Holland Paleosol in the upper part of dunes (Arbogast and Packman, 2004). Based on OSL and stratigraphic data from this study, it appears that the majority of eolian sand at Arcadia Dunes was deposited in the past millennium. Eolian sand deposition began ca. 1 ka at both Exposures 1 and 2 and continued until about 0.5 ka, when the dunes largely stabilized.

This study raises questions about how the record of eolian sand deposition at Arcadia Dunes compares to other perched dune fields in the region where buried soils occur (Snyder, 1985; Anderton and Loope, 1995; Loope and Arbogast, 2000). This comparison is complicated by the fact that earlier chronologies are based entirely on uncalibrated ^{14}C ages from organics in buried soils. To accurately test these temporal relationships, it was first necessary to standardize the OSL and ^{14}C time scales. The ^{14}C ages were first calibrated with CALIB 6.0 (Stuiver and Reimer, 1993) using the Reimer et al. (2009) calibration curve. Subsequently, 50 years were added to each age yielding a uniform time scale based on AD 2000 for comparison of radiocarbon and luminescence ages. This comparison is presented in Fig. 11 as a series of probability density distributions (ages in 1σ).

The temporal comparison between dune fields (Fig. 11) reveals several interesting trends that would otherwise be unseen if contrasting (OSL and uncalibrated ^{14}C) time scales were used. If such a comparison was made, as in Fig. 10 where uncalibrated ^{14}C ages from Sleeping Bear (Snyder, 1985) are included, it would appear that dune growth began at each site at about the same time. Calibration of the original ^{14}C data (Fig. 11) instead reveals that dune growth actually began ca. 1500 years earlier elsewhere in northwest Lower Michigan and at Grand Sable than it did at Arcadia. This difference can possibly

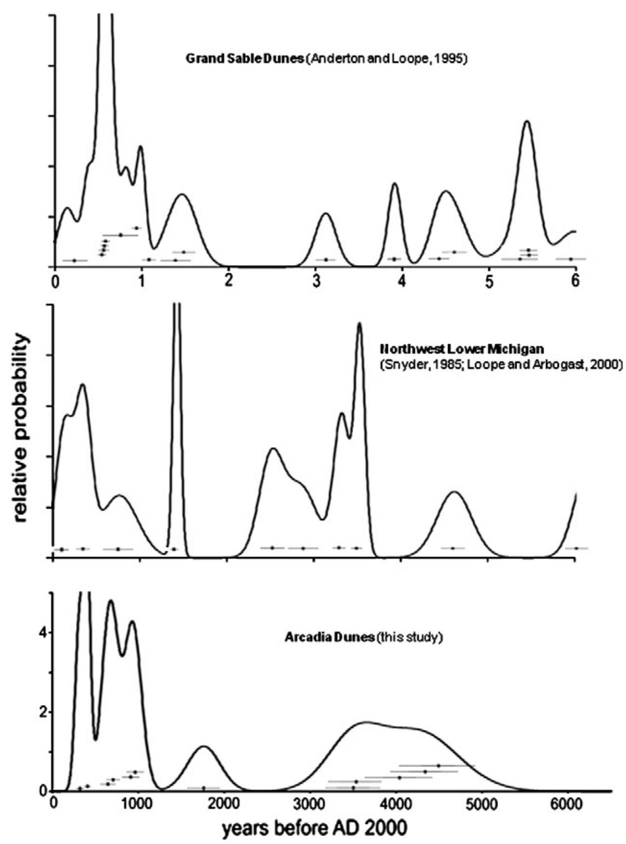

Figure 11. Comparison of Arcadia ages with calendar corrected data from perched dune fields in the region. Upper two panels show the probability density distributions (Singhvi et al., 2001) for radiocarbon-dated buried soils at Grand Sable dunes (Anderton and Loope, 1995) and northwest Lower Michigan (Snyder, 1985; Loope and Arbogast, 2000) and lower panel depicts probability density function for luminescence ages for Arcadia Dunes. All radiocarbon ages are calendar corrected (Stuiver and Reimer, 1993; Reimer et al., 2009) and then 50 years added, yielding a uniform time scale for comparison of radiocarbon and luminescence ages. Radiocarbon ages may predate eolian deposition by a few decades to a few hundred years because buried A horizons of spodic-type soils are reservoirs for carbon associated with degradation of organic material (Wang et al., 1996). The number, relative height of, and occurrence of peaks reflect mean values and associated errors of age estimates. Peaks defined by one or two ages may not be significant. This analysis indicates that there is broad chronologic consistency amongst records with eolian depositional event(s) ca. between 3.5 and 5 ka, 1.0 and 0.8 ka and 0.5 and 0.3 ka. A broad peak between 3.5 and 5.0 ka in the luminescence age plot may obscure multiple (2,3) eolian events because of the limited precision.

https://doi.org/10.1016/j.yqres.2012.01.006 Published online by Cambridge University Press

be explained by local variations in bluff position and composition between sites during the later stages of the Nipissing transgression and associated high stand. Or, conversely, eolian sand was supplied to dunes at Sleeping Bear and Grand Sable by sand driven upslope by waves as lake level rose toward the bluff base in the latter stages of the transgression, whereas it came directly from the bluff at Arcadia during the Nipissing high. Both methods of sand transport were proposed by Dow (1937).

Another interesting pattern occurs in the time between ca. 5 and 3 ka. At Grand Sable and other sites in northwest Lower Michigan, several distinct peaks in probability occur, whereas the distribution is broad for this interval at Arcadia. This dichotomy may exist in part because some of the ages at Arcadia bracket depositional intervals, whereas those elsewhere are from distinct soil horizons. It is also possible that peaks defined by one or two ages in the radiocarbon distributions may not be significant and/or that details of the depositional history at Arcadia are obscured because of limited OSL precision. Nevertheless, it appears that the period of time between 5.0 and 3.5 ka was an interval of dune growth at all perched dune fields.

The most obvious agreement in the chronologies occurs at ca. 1.0 ka, when the most extensive episode of dune growth occurred at Arcadia. Similar consistency between sites also occurs at ca. 0.8, 0.5, and 0.3 ka. This period of rapid dune growth is common along the Lake Michigan shoreline (e.g., Loope and Arbogast, 2000; Van Oort et al., 2001; Arbogast et al., 2002a; Hansen et al., 2002; Fisher and Loope, 2005; Lepczyk and Arbogast, 2005; Hansen et al., 2010), indicating that the supply of eolian sand was high along most of coast at this time.

Why did the supply of eolian sand dramatically increase at 1 ka after a lengthy hiatus? Past research on Lake Michigan coastal dunes (e.g., Loope and Arbogast, 2000; Arbogast et al., 2002a; Hansen et al., 2002; Fisher and Loope, 2005; Lepczyk and Arbogast, 2005; Hansen et al., 2010) focused largely on the role that lake-level fluctuations alone have had on eolian sand supply. It has been inferred that dunes on high bluffs and lower lake terraces accrete during high lake levels when wave erosion erodes and destabilizes coastal faces, resulting in the mobilization of eolian sand (e.g., Loope and Arbogast, 2000; Arbogast et al., 2002a). In this context, the onset of dune growth at ca. 1 ka may have begun with a high lake phase at about the same time (Argyilan et al., 2010).

Although the onset of renewed dune activation at 1 ka can be temporally linked to a high lake phase, uncertainty remains why this high lake stand resulted in extensive eolian deposition relative to previous high stages, when far less eolian sand was mobilized. In particular, the supply of eolian sand was significantly limited along the Lake Michigan coast between about 2.5 and 1 ka when several meter-scale lake-level fluctuations occurred, including a notable transgression and regression (Baedke and Thompson, 2000). This dichotomy suggests that the supply of eolian sand at Arcadia and other coastal sites may be also governed by variables other than lake-level fluctuations. One such factor may be the relationship of lakes Superior, Michigan and Huron, which were contiguous prior to dynamic separation of Lake Superior ca. 1.2 ka due to isostatic uplift (Johnston et al., 2007). Thus, higher lake stands ca. 4.5 to 1.2 ka resulted in a larger contiguous lake with greater volume and coastline to potentially dissipate wave energy, particularly with storms. Following separation of Lake Superior at ca. 1.2 ka, the coastal zone of an independent Lake Michigan/Huron may have been more susceptible to wave erosion; a documented effect in some Lake Superior standplains with separation of Lake Superior from lakes Michigan and Huron (Johnston et al., 2007).

Another potential factor in coastal dune reactivation is regional drought, though the upper Great Lakes is a rather mesic environment. Also, the ubiquity of Spodosol-like soils in the stratigraphic record is evidence of persistent conifer coverage in the late Holocene. Droughts in the Great Lakes can lead to a lowering in the water table (cf. Booth et al., 2006a), heightened direct mortality in coniferous forest and/or through insect infestation or fires. In this context, extensive dune growth between 1 and 0.5 ka at Arcadia and elsewhere occurred during a time when three major regional droughts were documented (Booth et al., 2006a). Similarly, a pair of droughts has also been observed at about 1.8 ka (Booth et al., 2006a) that correlate with an episode of higher eolian sand supply at Arcadia.

Although correlation does not equal causation, coastal dune formation between about 1 and 0.5 ka correlates with reactivation of dune fields in the Great Plains (e.g., Sridhar et al., 2006; Hanson et al., 2009, 2010), which has been attributed to an extensive megadrought during the Medieval Warm Period. This extended drought is associated with a distinct shift in the oceanic-atmosphere circulation in the Northern Hemisphere with persistent La Nina conditions in the Equatorial Pacific Ocean and a positive North Atlantic Oscillation which dramatically reduces precipitation in to mid-continental North America (e.g., Feng et al., 2008). In the Great Plains, dune mobilization during drought periods is clearly attributed to reduced vegetation and subsequent destabilization of dunes (e.g., Muhs and Maat, 1993; Arbogast, 1996; Sridhar et al., 2006; Hanson et al., 2009, 2010).

Climate model simulations indicate an about 10 to 20% reduction in precipitation in the Great Lakes area during the Medieval Warm Period (Feng et al., 2008), but it is unclear the response of forest biomes at Arcadia and other coastal dunes with such a reduction in precipitation. Groundwater table reconstructions show a modest drop during the Medieval Warm Period, significantly less than other drought periods in the past ca. 5 ka (Booth et al., 2006a). Alternatively, the rapid combination of both wet and dry extremes, particularly between about 1 and 0.5 ka (Booth et al., 2006a), may have caused dune growth, with increasing sand supply during wet times that was blown during subsequent dry spells. Thus, dune growth is related to lake-level fluctuations, but is triggered by rapidly occurring and complex climate extremes (Feng et al., 2008). Prevailing westerly winds were also apparently stronger during this interval of time (Booth et al., 2006b), which may be a critical factor.

Conclusion

Pedostratigraphic analysis, coupled with systematic OSL dating, identified numerous periods of landscape stability and eolian deposition at Arcadia Dunes during the late Holocene. A well-developed paleosol is formed in the uppermost part of underlying glacial deposits, which apparently reflects a period of landscape stability during the Chippewa low lake stage and the early part of the Nipissing transgression. Eolian sands subsequently buried this basal paleosol ca. 4.5 ka during the Nipissing high stand. The next period of dune growth occurred at ca. 3.5 ka during the post-Nipissing regression. Although lake level was falling overall, the period of 3.9 to 3.0 ka is characterized by decadal- to century-scale hydrologic variability, as documented in adjacent peatlands (Booth et al., 2006a).

Growth of the Arcadia dunes continued in the late Holocene with deposition at ca. 1.7 ka and between 1.0 ka and 0.5 ka. Most sand deposition occurred within the last 1000 years, which may reflect a concomitant high lake phase (Argyilan et al., 2010) and a potential change in lake hydrodynamics with final isostatic separation of Lake Superior from lakes Michigan and Huron (Johnston et al., 2007). Heightened sand availability may be also associated with decadal-scale hydrologic variability associated with the Medieval Warm Period (cf. Booth et al., 2006a), though this drought impacts on mesic environments of the Great Lakes is not well documented (e.g., Feng et al., 2008). Comparison of OSL age data from this study and calendar corrected ^{14}C ages from previous research indicates that dune growth at Arcadia began after it did in other perched dunes in the region. Otherwise, age comparisons indicate broad agreement in the chronology of eolian sand deposition between sites.

Acknowledgments

We thank the agencies and individuals who made this study possible including Xiomara Cordoba-Lepczyk, Brad Gerlach, and Glen Chown from the Grand Traverse Regional Land Conservancy for providing funding, resources, and access at Arcadia Dunes. We acknowledge the Department of Geography at Michigan State University for their funding and resources. Finally, we appreciate the efforts of Dr. Walter Loope (USGS) and an anonymous reviewer, who suggested several important changes that strengthened the manuscript.

References

Anderton, J.B., Loope, W.L., 1995. Buried Soils in a perched dunefield as indicators of Late Holocene lake-level change in the Lake Superior basin. Quaternary Research 44, 190–199.

Arbogast, A.F., 1996. Stratigraphic evidence for late-Holocene eolian sand mobilization and soil formation in south-central Kansas. Journal of Arid Environments 34, 403–414.

Arbogast, A.F., 2000. Estimating the time since final stabilization of a perched dune field along Lake Superior. The Professional Geographer 52, 594–606.

Arbogast, A.F., 2009. Sand Dunes. In: Schaetzl, R.J., Darden, J.T., Brandt, D. (Eds.), Michigan Geography and Geology. Pearson Custom Publishers, Upper Saddle River, NJ, pp. 274–287.

Arbogast, A.F., Loope, W.L., 1999. Maximum-limiting ages of Lake Michigan coastal dunes: their correlation with Holocene lake level history. Journal of Great Lakes Research 25, 372–382.

Arbogast, A.F., Packman, S.C., 2004. Middle-Holocene mobilization of aeolian sand in western upper Michigan and the potential relationship with climate and fire. The Holocene 14, 464–471.

Arbogast, A.F., Hansen, E.C., Van Oort, M.D., 2002a. Reconstructing the geomorphic evolution of large coastal dunes along the southeastern shore of Lake Michigan. Geomorphology 46, 241–255.

Arbogast, A.F., Wintle, A.G., Packman, S.C., 2002b. Widespread middle Holocene dune formation in the eastern Upper Peninsula of Michigan and the relationship to climate and outlet-controlled lake level. Geology 30, 55–58.

Arbogast, A.F., Shortridge, A.M., Bigsby, M.E., 2009. Using volumetric estimates of eolian sand to explain the geography of coastal sand dunes in Lower Michigan. Physical Geography 30, 479–500.

Argyilan, E.P., Forman, S.L., Johnston, J.W., Wilcox, D.A., 2005. Optically stimulated luminescence dating of late Holocene raised strandplain sequences adjacent to Lakes Michigan and Superior, Upper Peninsula, Michigan, USA. Quaternary Research 63, 122–135.

Argyilan, E.P., Forman, S.L., Thompson, T.A., 2010. Variability of Lake Michigan waterlevel during the past 1000 years reconstructed through optical dating of a coastal strandplain. The Holocene 20, 723–731.

Baedke, S., Thompson, T.A., 2000. A 4,700 year record of lake level and isostasy for Lake Michigan. Journal of Great Lakes Research 26, 416–426.

Bailey, S.D., Wintle, A.G., Duller, G.A.T., Bristow, C.S., 2001. Sand deposition during the last millennium at Aberffraw, Anglesey, North Wales as determined by OSL dating of quartz. Quaternary Science Reviews 20, 701–704.

Bauer, B.O., Sherman, D.J., 1999. Coastal dune dynamics: problems and prospects. In: Goudie, A.S., Livingstone, I., Stokes, S. (Eds.), Aeolian Environments. Sediments and Landforms, Wiley, New York, pp. 71–104.

Blewett, W.L., 1990. The glacial geomorphology of the Port Huron complex in northwestern Southern Michigan. Ph.D. dissertation. Michigan State University.

Booth, R.K., Notaro, M., Jackson, S.T., Kutzbachm, J.E., 2006a. Widespread drought episodes in the western Great Lakes in the past 2000 years: Geographic extent and potential mechanisms. Earth and Planetary Science Letters 242, 415–427.

Booth, R.K., Kutzbach, J.E., Hotchkiss, S.C., Bryson, R.A., 2006b. A reanalysis of the relationship between strong westerlies and precipitation in the Great Plains and Midwest regions of North America. Climatic Change 76, 427–441.

Bøtter-Jensen, L., Bulur, E., Duller, G.A.T., Murray, A.S., 2000. Advances in luminescence instrument systems. Radiation Measurements 32, 523–528.

Carter, R.W.G., Nordstrom, K.F., Psuty, N.P., 1990. The study of coastal dunes. In: Nordstron, K.F., Psuty, N.P., Carter, R.W.G. (Eds.), Coastal Dunes Form and Process. Wiley, New York, pp. 1–14.

Clemmensen, L.B., Pye, K., Murray, A., Heinemeir, J., 2001. Sedimentology, stratigraphy and landscape evolution of a Holocene coastal dune system, Lodbjerg, NW Jutland, Denmark. Sedimentology 48, 3–27.

Dow, K.W., 1937. The origin of perched dunes on the Manistee Moraine, Michigan. Michigan Academy of Science Arts and Letters 23, 427–440.

Duller, G.A.T., Botter-Jensen, L., Murray, A.S., 2003. Combining infrared and green-laser stimulation sources in single-grain luminescence measurements of feldspar and quartz. Radiation Measurements 37, 543–550.

Evenson, E.B., Farrand, W.R., Eschman, D.F., Mickelson, D.M., Maher, L.J., 1976. Greatlakean Substage: A Replacement for Valderan Substage in the Lake Michigan basin. Quaternary Research 6, 411–424.

Fain, J., Soumana, S., Montret, M., Miallier, D., Pilleyre, T., Sanzelle, S., 1999. Luminescence and ESR dating-Beta-dose attenuation for various grain shapes calculated by a Monte-Carlo method. Quaternary Science Reviews 18, 231–234.

Farrand, W., 1988. Glacial Lakes around Michigan. Michigan Department of Environmental Quality, Geological Survey Division, Lansing, MI.

Farrand, W.R., and Bell, D.L., 1982. Quaternary Geology of Michigan (Map). Michigan Department of Natural Resources-Geological Survey.

Feng, S., Oglesby, R.J., Rowe, C.M., Loope, D.B., Hu, Q., 2008. Atlantic and Pacific SST influences on Medieval drought in North America simulated by the Community Atmospheric Model. Journal of Geophysical Research-Atmospheres 113 (D11). doi:10.1029/2007JD009347.

Fisher, T.G., Loope, W.L., 2005. Aeolian sand preserved in Silver Lake: A new signal of Holocene high stands of Lake Michigan. The Holocene 15, 1072–1078.

Forman, S.L., Gomez, J., Marin, L., Webb, R., Miller, G.H., 2001. Deciphering eolian sand depositional records from the western Great Plains. In: Overpeck, J., Trenberth, K. (Eds.), Proceedings of the CLIVAR/PAGES/IPCC Workshop: A multi-millennial perspective on drought and implications for the future. Tucson, AZ, 2003.

Forman, S.L., Nordt, L., Gomez, J., Pierson, J., 2009. Late Holocene dune migration on the south Texas sand sheet. Geomorphology 108, 159–170.

Galbraith, R.F., Roberts, R.G., Laslett, G.M., Yoshida, H., Olley, J.M., 1999. Optical dating of single and multiple grains of quartz from jinmium rock shelter, northern Australia, part 1, Experimental design and statistical models. Archaeometry 41, 339–364.

Gares, P.A., Nordstrom, K.F., 1995. A cyclic model of foredune blowout evolution for a leeward coast: Island Beach, New Jersey. Annals of the Association of American Geographers 85, 1–20.

Hansen, E.C., Arbogast, A.F., Packman, S.C., Hansen, B., 2002. Post-Nipissing origin of a backdune complex along the southeastern shore of Lake Michigan. Physical Geography 23, 233–244.

Hansen, E.C., Fisher, T.G., Arbogast, A.F., Bateman, M., 2010. Geomorphic history of low perched, transgressive dune complexes along the southeastern shore of Lake Michigan. Aeolian Research 1, 111–127.

Hanson, P.R., Joeckel, R.M., Young, A.R., Horn, J., 2009. Late Holocene dune activity in the Eastern Platte River Valley, Nebraska. Geomorphology 103, 555–561.

Hanson, P.R., Arbogast, A.F., Johnson, W.C., Joeckel, R.M., Young, A.R., 2010. Megadroughts and late Holocene dune activation at the eastern margin of the Great Plains, north-central Kansas, USA. Aeolian Research 1, 101–110.

Hesp, P.A., 2001. The Manawatu Dunefield: Environmental change and human impacts. New Zealand Geographer 57, 33–40.

Holmes, P.J., Barker, C.H., Bateman, M.D., Thomas, D.S.G., Telfer, M.W., Lawson, M.P., 2008. A Holocene-late Pleistocene aeolian record from lunette dunes of the western Free State panfield, South Africa. The Holocene 18, 1193–1205.

Johnston, J.W., Thompson, T.A., Wilcox, D.A., Baedke, S.J., 2007. Geomorphic and sedimentologic evidence for the separation of Lake Superior from Lake Michigan and Huron. Journal of Paleolimnology 37, 349–364.

Kroell III, M.L., 2008. Soil Survey of Benzie and Manistee Counties, Michigan. United States Department of Agriculture Soil Conservation Service, U.S. Government Printing Office, Washington, D.C.

Larson, G., Schaetzl, R.J., 2001. Origin and evolution of the Great Lakes. Journal of Great Lakes Research 27, 518–546.

Lepczyk, X.C., Arbogast, A.F., 2005. Geomorphic history of dunes at Petoskey State Park, Petoskey, Michigan. Journal of Coastal Research 21, 231–241.

Leverett, F., Taylor, F.B., 1915. The Pleistocene of Indiana and Michigan and the history of the Great lakes. United States Geological Survey Monograph, 53. U.S. Government Printing Office, Washington, D.C. 529 pp.

Loope, W.L., Arbogast, A.F., 2000. Dominance of an 150-year cycle of sand-supply change in late Holocene dune-building along the eastern shore of Lake Michigan. Quaternary Research 54, 414–422.

Martinho, C.T., Hesp, P.A., Dillenburg, S.R., 2010. Morphological and temporal variations of transgressive dunefields of the northern and mid-littoral Rio Grande do Sul coast, Southern Brazil. Geomorphology 117, 14–32.

Mejdahl, V., Christiansen, H.H., 1994. Procedures used for luminescence dating of sediments. Boreas 13, 403–406.

Muhs, D.R., Maat, P.B., 1993. The potential response of eolian sands to greenhouse warming and precipitation reduction on the Great Plains of the U.S.A. Journal of Arid Environments 25, 351–361.

Murray, A.S., Wintle, A.G., 2003. The single aliquot regenerative dose protocol: potential for improvements in reliability. Radiation Measurements 37, 377–381.

Prescott, J.R., Hutton, J.T., 1994. Cosmic ray contributions to dose rates for luminescence and ESR dating: large depths and long-term time variations. Radiation Measurements 23, 497–500.

Reimer, P.J., Baillie, M.G.L., Bard, E., Bayliss, A., Beck, J.W., Blackwell, P.G., Bronk, R.C., Buck, C.E., Burr, G.S., Edwards, R.L., Friedrich, M., Grootes, P.M., Guilderson, T.P., Hajdas, I., Heaton, T.J., Hogg, A.G., Hughen, K.A., Kaiser, K.F., Kromer, B., McCormac, F.G., Manning, S.W., Reimer, R.W., Richards, D.A., Southon, J.R., Talamo, S., Turney, C.S.M., van der Plicht, J., Weyhenmeyer, C.E., 2009. IntCal09 and Marine09 radiocarbon age calibration curves, 0–50,000 years cal BP. Radiocarbon 51, 1111–1150.

Roberts, H.M., Plater, A.J., 2007. Reconstruction of Holocene foreland progradation using optically stimulated luminescence (OSL) dating: an example from Dungeness, UK. The Holocene 17, 495–505.

Short, A.D., 2010. Sediment transport around Australia - Sources, mechanisms, rates, and barrier forms. Journal of Coastal Research 26, 395–402.

Singhvi, A.K., Bluszcz, A., Bateman, M.D., Rao, M.S., 2001. Luminescence dating of loess-palaeosol sequences and coversands: methodological aspects and palaeoclimatic implications. Earth-Science Reviews 54, 193–211.

Snyder, F.S., 1985. A spatial and temporal analysis of the Sleeping Bear Dunes complex, Michigan (A contribution to the geomorphology of perched dunes in humid continental regions). Ph.D. dissertation. University of Pittsburgh.
Sridhar, V., Loope, D.B., Swinehart, J.B., Mason, J.A., Oglesby, R.J., Rowe, C.M., 2006. Large wind shift on the Great Plains during the Medieval Warm Period. Science 313, 345–347.
Stuiver, M., Reimer, P.J., 1993. Extended ^{14}C data base and revised CALIB 3.0 ^{14}C age calibration program. Radiocarbon 35, 215–230.
Tamura, T., Bateman, M.D., Kodama, Y., Saitoh, Y., Watanabe, K., Yamaquchi, N., Matsumoto, D., 2011. Building of shore-oblique transverse dune ridges revealed by ground-penetrating radar and optical dating over the last 500 years on Tottori coast, Japan Sea. Geomorphology 132, 153–166.
Thompson, T.A., Baedke, S.J., 1999. Strandplain evidence for reconstructing late Holocene lake level in the Lake Michigan Basin. In: Sellinger, C.E., Quinn, F.H. (Eds.), Proceedings of the Great Lakes Paleo-Levels Workshop: The Last 4000 years. Great Lakes Environmental Research Laboratory, NOAA Technical Memorandum ERL GLERL-113, pp. 30–34. August, 1999.
Van Oort, M., Arbogast, A.F., Hansen, E.C., Hansen, B., 2001. Geomorphological history of massive parabolic dunes, Van Buren State Park, Van Buren County, Michigan. Michigan Academician 33, 175–188.
Walker, I., Hesp, P.A., Davidson-Arnott, R., Ollerhead, J., 2006. Topographic steering of alongshore flow over a vegetated foredune: Greenwich dunes, Prince Edward Island, Canada. Journal of Coastal Research 22, 1278–1291.
Wang, Y., Amundson, R., Trumbore, S., 1996. Radiocarbon dating of soil organic matter. Quaternary Research 45, 282–288.